

Beta-Band Frequency Peaks Inside the Subthalamic Nucleus as a Biomarker for Motor Improvement After Deep Brain Stimulation in Parkinson's Disease

Konstantinos P. Michmizos, *Member, IEEE*, Polytimi Frangou, *Student Member, IEEE*, Pantelis Stathis, Damianos Sakas, and Konstantina S. Nikita, *Senior Member, IEEE*

I. INTRODUCTION

Abstract—Deep brain stimulation (DBS) of the subthalamic nucleus (STN) remains an empirical, yet highly effective, surgical treatment for advanced Parkinson's disease (PD). DBS outcome depends on accurate stimulation of the STN sensorimotor area which is a trial-and-error procedure taking place during and after surgery. Pathologically enhanced beta-band (13–35 Hz) oscillatory activity across the cortico-basal ganglia pathways is a prominent neurophysiological phenomenon associated with PD. We hypothesized that weighing together beta-band frequency peaks from simultaneous microelectrode recordings in “off-state” PD patients could map the individual neuroanatomical variability and serve as a biomarker for the location of the STN sensorimotor neurons. We validated our hypothesis with 9 and 11 patients that, respectively, responded well and poorly to bilateral DBS, after at least two years of follow up. We categorized “good” and “poor” DBS responders based on their clinical assessment alongside a $> 40\%$ and $< 30\%$ change, respectively, in “off” unified PD rating scale motor scores. Good (poor) DBS responders had, in average, 1 mm (3.5 mm) vertical distance between the maximum beta-peak weighted across the parallel microelectrodes and the center of the stimulation area. The distances were statistically different in the two groups ($p = 0.0025$). Our biomarker could provide personalized intra- and postoperative support in stimulating the STN sensorimotor area associated with optimal long-term clinical benefits.

Index Terms—Beta-band oscillations, clinical biomarker, deep brain stimulation (DBS), neuromodulation, Parkinson's disease (PD).

Manuscript received January 4, 2014; revised June 13, 2014; accepted July 21, 2014. Date of publication July 30, 2014; date of current version December 30, 2014.

K. P. Michmizos is with the Martinos Center for Biomedical Imaging, Massachusetts General Hospital, Boston, MA 02114 USA; the Department of Neurology, Harvard Medical School, Boston, MA 02115 USA; the McGovern Institute for Brain Research, Massachusetts Institute of Technology, Cambridge, MA 02139 USA (e-mail: konmic@mgh.harvard.edu).

P. Frangou is with the Adaptive Brain Laboratory, Department of Psychology, University of Cambridge, Cambridge CB2 1TN, U.K. (e-mail: pf319@cam.ac.uk).

P. Stathis is with the Department of Neurology, Mediterraneo Hospital, Athens 16675, Greece and also with the Department of Neurosurgery, “Evangelismos” General Hospital, National and Kapodistrian University of Athens, Athens 11527, Greece (e-mail: stathis.pantelis@gmail.com).

D. Sakas is with the Department of Neurosurgery, “Evangelismos” General Hospital, National and Kapodistrian University of Athens, Athens 11527, Greece (e-mail: sakasde@med.uoa.gr).

K. S. Nikita is with the Biomedical Simulations and Imaging Laboratory, Faculty of Electrical and Computer Engineering, National Technical University of Athens, Athens 10682, Greece (e-mail: knikita@ece.ntua.gr).

Color versions of one or more of the figures in this paper are available online at <http://ieeexplore.ieee.org>.

Digital Object Identifier 10.1109/JBHI.2014.2344102

ALTHOUGH deep brain stimulation (DBS) of the subthalamic nucleus (STN) is being used in Parkinson's disease (PD) for two decades [1], the theoretical knowledge of the underlying therapeutic mechanisms is still surpassed by its clinical results [2]. STN-DBS provides consistent clinical benefits, such as alleviation of Parkinsonian resting tremor, rigidity, and bradykinesia [3], and reduces dopamine replacement requirements by 50% to 60% [4]. Its major pitfall though is that good clinical results and adverse side effects mainly depend on the accurate implantation of the stimulation electrode within the sensorimotor area of the STN [5], [6].

During DBS implantation, the precise placement of the stimulation electrode is macroscopically guided by microelectrode mapping of the neuronal activity at different subcortical depths inside and outside the STN [7]. An expert neurologist monitors microelectrode recordings (MERs) to identify the characteristic spontaneous discharge pattern of the STN and of surrounding nuclei as well as the locations of the movement-related STN neurons [8]. The microelectrode trajectory that is selected for stimulation is the one exhibiting movement-related activity or the largest amount of STN-specific discharge pattern. Once the trajectory is selected, a “trial-and-error” macrostimulation determines the therapeutic window for the selected STN area by identifying the best clinical response without intraoperative side effects [9].

The STN target identification through microelectrode mapping does not always secure a good clinical outcome [7], [10]. The intraoperative functional tests that are conducted while the patient lies down on the operating table, during “off-state”, can give only a gross estimation of the target location and, therefore, of the clinical improvement. What is more, the substantial amelioration of PD symptoms such as dyskinesias as well as sensory and cognitive side effects occur in the further postoperative course [5], [11]. Nonetheless, there is no *functional biomarker* that can currently relate, during the operation, the stimulated STN area with the *long-term* DBS outcome.

Recording the neuronal activity as close to its generator as possible allows maxima spatial resolution and accuracy for a MER-based localization of the STN. High frequency components of MERs (mainly the background noise and spike count) have been used by several studies to detect the borders of the STN [12]–[14]. The low frequency component of MERs, named as local field potential (LFP), is also an information-rich signal.

We have developed LFP-driven models that simulate the STN spike activity [15]–[18] and the effects of DBS, at the neuronal level [19]. LFPs have also been used for the localization of the STN and of adjacent regions such as the zona incerta [20], [21]. The STN detection became even more prominent when the focal nature of certain band activities in the STN-LFP was revealed. The interrelationship between the emergence of oscillations and synchrony among STN neurons in “off-state” PD patients [22], [23] further spurred studies on the increased power and coherence in the alpha and beta frequency bands, in these patients [24], [25]. Specifically for beta-band frequencies, accumulated evidence suggests a persistent relation between good clinical response to STN-DBS and a significant *attenuation in beta-band LFP power*, at rest [26], [27].

In an effort to detect intraoperatively the STN borders, several online algorithms fuse multiple features from a single MER. For example, Zaidel *et al.* combine the background noise level with spectrum estimation to detect the oscillatory dorsolateral region (seemingly the preferred location for STN-DBS [28]) and nonoscillatory subterritories within the STN [14]. Recently, Cagman *et al.* introduced an automated algorithm that combines knowledge of background noise level, compound firing rate, and power spectral density (PSD) along each trajectory to detect the dorsal and the ventral borders of the STN [29]. These studies rely on features acquired from a single microelectrode to distinguish the STN from the neighboring structures. However, due to different disease states or presence of artifacts, changes in the MER features specific to the STN can show significant variation. Importantly, the anatomical localization of the dorsolateral region of the STN and its stimulation does not always provide a positive therapeutic long-term response for STN-DBS [30]. To overcome the pitfalls, one potential approach, which is proposed in this study, is to combine the information about the *individual neuroanatomical variability* from adjacent microelectrodes.

In this paper, we hypothesized that beta-frequency amplitude peaks corresponded to the richest, in beta oscillations, motor territories of the STN; we further hypothesized that the *distance* between the stimulation and the STN sensorimotor areas determined the long-term clinical efficacy of DBS. Although such an assumption remains to be neurophysiologically verified, herein we propose a weighted sum of spontaneous beta-band peaks across the MERs as a functional biomarker of DBS efficacy. We validated our marker by comparing the proposed stimulation locations with the clinical decisions of a human expert in 20 PD patients (9 that responded well to therapy and 11 that did not), with at least two years of follow up after the DBS implantation. We found that the distance between the beta-band marker and the center of the stimulation area could predict the DBS efficacy. Our results build support for using beta-band peaks to inform the optimal localization of the stimulation points inside the STN, during DBS implantation.

II. METHODS

A. MERs and DBS Implantation

The patients underwent surgery during “off” state according to the CAPSIT-PD protocol [31] and gave informed consent

according to the procedure approved by the Ethics and Institutional Review Board committee of Evaggelismos Hospital, Athens, Greece. We identified target coordinates after fusing CT and intraoperative imaging with 3-D MRI images using the Radionics Stereoplan workstation. The five microelectrode trajectories were positioned in a cross (ben gun) formation (central, anterior, posterior, lateral, and medial) and recordings lasted for 10 s. The central electrode had a 2 mm distance from any electrode in the periphery. The MERs typically initiated at 5 mm above the STN target and sampled the neuronal activity across the electrode descent. They were obtained at 0.5 mm steps through the STN to the substantia nigra reticulata using the Leadpoint Neural Activity Monitoring System (Medtronic, Inc., Minneapolis, MN). For each electrode depth, an expert neurologist (coauthor of this study, P.S.) identified the characteristic STN discharge pattern and the movement related activity during voluntary or passive movements of the patient. Intraoperative clinical assessment of the patient was performed during current stimulation (0.5–5.0 V, 60- μ s pulse width, 130 Hz).

Upon the frame-based stereotactic localization of the target, we implanted the Navigus (Image-guided Neurologics, Melbourne, FL) cranial base and the cap lead-anchoring device over the burr hole and secured it with two self-tapping screws. After carefully inserting the stimulation lead to the target, we verified proper lead positioning with intraoperative fluoroscopy (lateral skull X-rays). We then removed the stylet of the lead and secured the distal shaft of the implanted lead into the Navigus device. The pulse generator was connected to the distal end of the implanted lead and secured into the implanted ferrule. After closing the scalp wound in anatomical layers, we removed the supportive head frame and, under general anesthesia, we placed the pulse generator. On the third day after surgery, the patient underwent postoperative MRI for further verification of the lead position [32]. This procedure secured that only downward displacement of the stimulation lead could be present that could not exceed 1.5 mm [9], [33].

Stimulation parameters (contact, pulse amplitude, width, and frequency) were setup one week after surgery according to a standard protocol [34] for optimal clinical benefit. The quadripolar stimulation electrodes (Medtronic leads) were stereotactically implanted into the STN of both sides. Contact-to-contact distance was 0.5 mm whereas the contact itself had a diameter of 1.5 mm. Stimulation was either monopolar or bipolar (i.e., two contacts with the same negative polarity).

B. Data Processing and Analysis

The MERs were acquired from spontaneous STN activity, defined as the neuronal activity acquired during periods in which the PD patient lied down immobile on the operating table. No electrical stimulation was applied during recordings. Neither active nor passive movements were executed during the analyzed MERs. Only signals with STN activity present were included in this study. Signals were visually inspected by an expert neurologist (P. S) using the Leadpoint Export Utility software (Medtronic), after the follow-up period of at least two

TABLE I
PATIENTS WITH GOOD RESPONSE TO DBS

Subject (H & Y)	UPDRS pre/post On-state	UPDRS pre/post Off-state	Levod. Equiv. pre/post (mg)	Stimulation contact
G1	40	75	1400	P [-4, -2.5]
(3)	32	38	500	M [-5, -3.5]
G2	28	60	1500	C [-1.5, 0]
(2.5)	20	35	550	A [-1.5, 0]
G3	26	66	1400	C [2, 3.5]
(3)	24	28	450	P [-0.5, 1]
G4	32	70	1800	P [-0.5, 3] *
(3)	30	41	750	P [-1.5, 2] *
G5	26	61	1100	L [-4, 2.5]
(2.5)	18	24	300	P [-1.5, 0]
G6	30	78	1650	P [-4, -0.5] *
(3)	26	48	750	M [-3, -1.5]
G7	34	75	750	C [-1.5, 0]
(3)	30	44	450	C [-2.5, -1]
G8	16	52	1450	C [-2.5, -1]
(2.5)	8	18	600	A [-2, -0.5]
G9	38	75	1700	C [-5.5, -4]
(3)	22	32	600	L [-6, -2.5] *

Column 1: first (second) line corresponds to Subject ID and Hoehn and Yahr (H&Y) PD scale for disease progression, respectively; Columns 2-4: first (second) line corresponds to pre- (post-) surgery clinical measures; Column 5: first (second) line corresponds to left (right) stimulation contact [C: Central, P: Posterior, A: Anterior, M: Medial, L: Lateral electrodes]; * denotes activation of two stimulation contacts.

TABLE II
PATIENTS WITH POOR RESPONSE TO DBS

Subject (H & Y)	UPDRS pre/post On-state	UPDRS pre/post Off-state	Levod. Equiv. pre/post (mg)	Stimulation contact
P1	16	45	1250	P [-5.5, -2] *
(3)	18	38	750	M [-5, -1.5] *
P2	22	64	1500	C [-5.5, -2] *
(2.5)	19	43	750	M [-4.5, -3]
P3	34	61	1150	M [-3.5, -2]
(3)	30	54	850	L [-3.5, 0] *
P4	28	77	1000	P [-2.5, -1]
(3)	24	56	600	C [-4.5, -3]
P5	40	68	2300	C [-4.5, -3]
(3.5)	38	66	1800	M [-1.5, 0]
P6	42	73	880	A [-3, -1.5]
(3)	38	66	800	C [-1.5, 0]
P7	32	76	600	M [-6, -4.5]
(2)	24	62	450	P [-6.5, -5]
P8	32	78	1050	A [-3, -1.5]
(3)	26	64	750	C [-1.5, 0]
P9	62	83	850	A [-4.5, -3]
(2.5)	57	68	750	C [-5.5, -4]
P10	23	55	1600	C [-5.5, -4]
(2.5)	19	37	850	M [-3.5, -2]
P11	18	42	950	C [-5.5, -2] *
(3)	9	32	650	M [-1.5, 2] *

Annotations as in Table I.

years. Offline data processing and analysis were conducted with MATLAB (The MathWorks, MA, USA). Each 24 kHz signal was first low-pass filtered, using an equiripple filter with a cut-off frequency of 6 kHz, order of 900 and peak to peak (p-p) rippling equal to 1.6×10^{-5} dB and then down-sampled to 12 kHz for computational convenience. PSD estimation for each frequency, k , was done using the Welch's method [35] that divides the sampled data, f_n , into Q overlapping blocks of length K , and estimates the periodogram of each block:

$$I_K^{(q)}(k) = \frac{1}{KU} \sum_{n=0}^{K-1} f_n w(n) e^{-j2\pi nk/Q}, \quad q = 1, \dots, Q \quad (1)$$

where

$$U = \frac{1}{K} \sum_{n=0}^{K-1} w^2(n) \quad (2)$$

accounts for the power reduction due to the windowing operation and allows the estimator to be asymptotically unbiased, and $w(n)$ is the Bartlett window. We kept the data window equal to 0.68 s and the overlap between windows to 50% and estimated the PSD as the ensemble average of the windowed and overlapped blocks:

$$\bar{I}_K(k) = \frac{1}{Q} \sum_{q=1}^Q I_K^{(q)}(k). \quad (3)$$

The beta-band peak was a prominent amplitude spike in PSD at the range of 13–35 Hz; for typical examples of beta-band peaks, see [36, Fig. 3(b) and (d)].

To assess normality of data, we reinforced our visual inspection of the distributions with the D'Agostino-Pearson's omnibus K^2 test [37], under the null hypothesis that normality is a reasonable assumption regarding the population distribution of a random sample that was not skewed or suffered from kurtosis. After confirming that the null hypothesis could not be rejected at the significance level of 0.05, we employed the t -test to compare the means between the grouped samples.

C. Postoperative Follow up of DBS Patients

Twenty patients were recruited for this study. They were grouped into two categories, namely the “good” responders and the “poor” responders. We categorized the patients after clinical assessment in accordance with follow up studies in PD patients [38], [39] that are based on standard neurological evaluations pre- and post operatively, namely the unified Parkinson's disease rating scale (UPDRS), the daily dose of anti-Parkinsonian medication in levodopa equivalents and the Hoehn and Yahr PD scale for disease progression [40] (Tables I and II). In addition to following a common clinical practice, our selection of “poor” and “good” DBS responders was consistent with a $< 30\%$ and $> 40\%$ change in the “off-state” UPDRS after the DBS surgery. The “off-state” UPDRS change has been used successfully in prior studies to discriminate between “good” and “poor” responders [41], [42].

During the follow up, the neurologist had no access to the information acquired from the MER data (beta-band peaks). Hence, the final contact selection was clinical in nature. In one patient with poor clinical outcome (P8), a second contact ([-5.0, -3.5]) was added to the first one ([-3.0, -1.5]) during a follow-up visit, that patient also developed dysarthria. One patient who was allocated to “good” responders (G9) improved

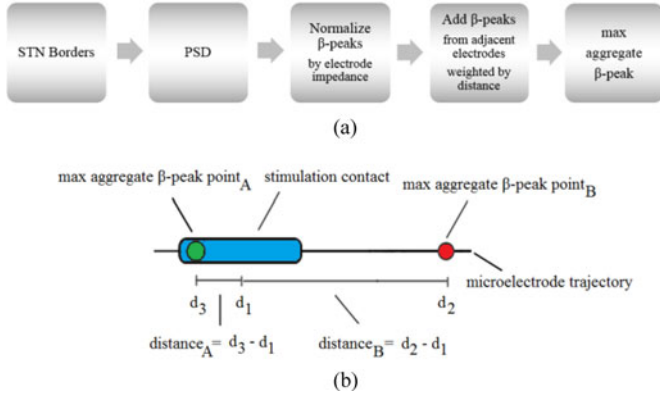


Fig. 1. (a) Flowchart for estimating the proposed biomarker at depth d and microelectrode i . After STN border detection, the PSD was estimated and the beta peak (β peak) was normalized by the microelectrode impedance, Z_i . The beta peaks were weighed by their distance, WD_i , and were added together to estimate the maximum peak for each depth and microelectrode i . (b) Marker validation: the distance between the max beta peak and the center of the stimulation contact (cyan rectangle). When the maximum aggregate beta peak was below the stimulation contact (point_A, green circle), the distance was positive; otherwise (e.g. point_B, red circle), the distance was negative.

significantly in tremor and dyskinesia but not in rigidity and walking ability and further developed a partially stimulation-dependent dysarthrophonia.

D. Weighted Summation of Aggregate Normalized Beta Peak as a Neurophysiological Biomarker

The estimation of the proposed biomarker for a given electrode depth is shown in Fig. 1(a). Upon defining the STN borders, $d_i \in [LB_i, UB_i]$ mm where LB_i and UB_i are, respectively, the lower and upper STN boundaries for each microelectrode trajectory, $i \in [1, \dots, 5]$, we estimated the power spectrum for each depth, PSD_i^d , and normalized the beta-band peaks, β_i^d by the microelectrode impedance, Z_i :

$$\bar{\beta}_i^d = \frac{\beta_i^d}{Z_i}. \quad (4)$$

We then added the normalized same-depth beta peaks across electrodes, weighed by their distance to the electrode of reference:

$$W_i^d = \bar{\beta}_i^d + \sum_{\substack{m=1, \\ m \neq i}}^5 \bar{\beta}_m^d \cdot WD_m \quad (5)$$

where $WD_i = 1/L$ is the weight related to the distance between the adjacent microelectrodes and microelectrode i , and $L \in \{2, 2\sqrt{2}, 4\}$ mm corresponds to the Euclidean distance between the two microelectrodes (see Section II-A for interelectrode distance). For beta frequencies, this is in agreement with current models of low-pass filtering of LFPs in brain tissue (see [43, Figs. 4 and 10]). We then estimated our proposed marker, m , as follows:

$$m = \max_i(\max_d(W_i^d)). \quad (6)$$

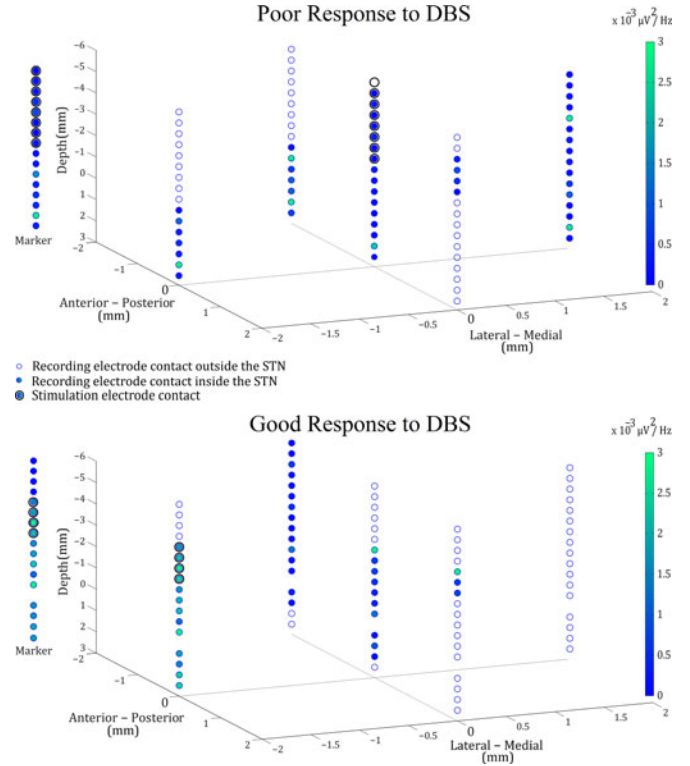


Fig. 2. Typical examples for poor (top) and good (bottom) responses to DBS treatment. The marker is shown on the left of each plot. In poor response (P2), there is a 5.75 mm distance between the maximum aggregate β -peak marker, m , and the center of the stimulation area. Note the prominent β -peaks observed in all four microelectrodes that were inside the STN at a 2 mm depth. In good response (G5), the maximum aggregate β -peak marker fell inside the stimulation area; other prominent β -peaks in Central and Posterior electrodes were at -3 mm and -4 mm depths, respectively; both depths were inside the stimulation area at depths between $[-4, -2.5]$ mm.

To validate our marker, we calculated its distance from the center of the stimulation electrode [see Fig. 1(b)].

III. RESULTS

A comparison across the “good” and “poor” groups showed that although they started from the same baseline (t -test on off-state, preoperative UPDRS; $p = 0.66$, $t_{\text{stat}} = 0.45$, $df = 18$, $SD = 11.7$), the clinical outcome after DBS differed significantly (t -test on off-state, postoperative UPDRS; $p = 0.002$, $t_{\text{stat}} = -3.55$, $df = 18$, $SD = 11.9$). For each hemisphere we tested, there was at least one trajectory with at least one beta peak inside the STN. The beta peak with the highest amplitude across microelectrodes was found in the trajectory that was intraoperatively selected for stimulation, in 13 out of 18 STN of “good” responders and 16 out of 22 STN of “poor” responders. Our proposed marker was located inside (or at the tip of) the stimulation contact that gave optimal clinical result for 10 “good” response STN (see Fig. 2). The marker had a distance of no larger than 2 mm in at least one hemisphere for all “good” responders, with subject G9 being an exception. Two equivalent beta peaks in the weighted sum were usually related to bimonopolar stimulation. For “poor-response” patients, the marker had a distance of at least 2 mm in at least one of their hemispheres,

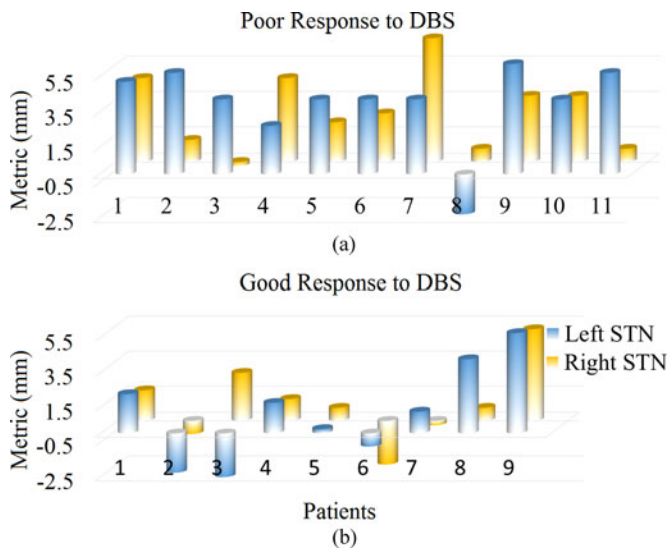


Fig. 3. Distance in millimeter between the beta-band peak and the center of the stimulation electrode for (a) “poor” and (b) “good” responders to DBS.

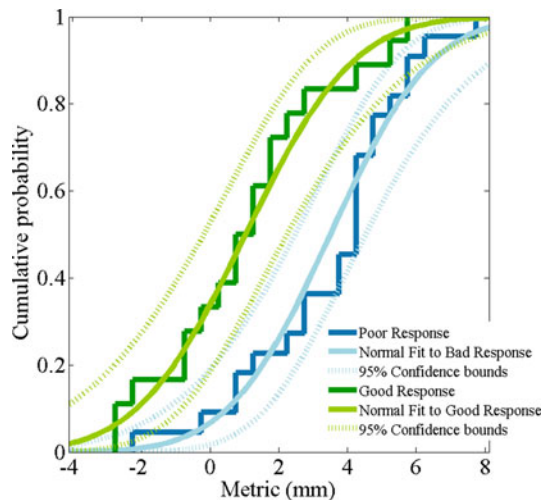


Fig. 4. Empirical and theoretical (normal best fit) cumulative distributive functions for “poor” and “good” response metrics. Distances in the two groups were found to be statistically significant (t -test, $p = 0.0025$). Best fit estimates for “poor” response data: μ (se) = 3.5 (0.49), σ (se) = 2.33 (0.36) and for “good” response data: μ (se) = 1.02 (0.58), σ (se) = 2.47 (0.43).

with subject P8 being an exception. The mean (SEM) distance was 3.5 (0.97) mm and 1.0 (1.14) mm for “poor” and “good” responders, respectively (see Fig. 3). The visual comparison of the empirical and the theoretical (best normal fit) distributions of the metrics (see Fig. 4) was reinforced by a student’s t -test that proposed a statistically significant difference in the distances between the center of the stimulation area and the proposed marker in the two groups of patients ($p = 0.0025$). Interestingly, no statistical difference was found in the amplitude of the weighted aggregate beta peak between the two groups ($p > 0.9$).

IV. DISCUSSION

The *long-term* clinical outcome of STN-DBS, at least in terms of a clustering of “poor” and “good” responders based on the change in the off-state UPDRS, seems to be predicted by the distance between the aggregate normalized beta peaks acquired during the DBS implantation surgery. In our dataset, we found that there was always an area of beta-band oscillations inside the STN that, depending on the patient, was a distinct area or not. This finding seems consistent with the hypothesis of *beta-band islands* that seem to exist, at least in some patients, in STN areas other than the dorsolateral area that one expects to find sensorimotor activity (see [44, Fig. 1]). This speculation could be reinforced by a functional organization model of the STN (see [23, Fig. 9]) and a recent study on the spatially distributed synchronizations as a key feature of STN pathophysiology in Parkinsonian tremor [45]. In these studies, STN neurons are also found to be clustered in high- and tremor-frequency patches that are interweaved with nonoscillatory neurons; an indication of different local functional neuronal organizations inside the STN. If this hypothesis is true, then the “poor” responders might benefit from placing a stimulation contact close to the other neuronal areas exhibiting prominent beta oscillations (see Fig. 2).

Mounting evidence suggests that beta-band oscillations are related to the sensorimotor neurons exhibiting pathophysiological synchronization inside the STN and other brain structures. A recent focus on the exaggerated beta-band (13–35 Hz) oscillations located in the cortico-basal ganglia pathways in patients with “off-state” PD [46] paved the way for this activity to be related to slowness and stiffness in PD [47] which are dominant features in movement assessment clinical metrics such as the UPDRS scale we estimated pre- and postoperatively (see Tables I and II). We speculate that the amplitude of the beta peak could be related to the level (or extent) of beta synchronization, either locally (within the STN) or in the long range. In that sense, the similar preoperative UPDRS levels between “good” and “poor” responders were consistent with our finding of similar amplitudes in the weighed aggregate beta peak acquired intraoperatively, across groups. In addition, we found no relationship between: 1) the oscillation frequency and the electrode location; and 2) the electrode location and the DBS outcome. These findings are consistent with a recent study suggesting that the topography of the low- (10–20 Hz), and high- (20–35 Hz) beta band does not differ in the STN [48] and another concluding that “coordinate-based lead location does not predict Parkinson’s disease deep brain stimulation outcome” [30].

The beta-peak metric was not available to the expert neurologist during follow up; his only guidance was the clinical symptoms of the patients. On one hand, our proposed beta-band marker was, in average, 1 mm away from the stimulation center in the “good” responders providing further evidence for DBS clinical results being associated with inhibition of beta oscillations [26], [27]. On the other hand, “poor” DBS responses are clinically associated with a narrow therapeutic window, i.e., a small range of stimulation currents that can provide effective therapy without causing side effects. To speculate further, the large (3.5 mm in average) difference between the beta marker

and the center of stimulation area in the “poor” responders might have prohibited the increase of the stimulation current up to a therapeutic level due to the side effects that arose from stimulating the STN areas between the DBS contact and the beta marker.

The failures of the beta-band marker to fully comply with the clinical outcome for 3 out of 20 PD patients could have a neurophysiological explanation related to the asymmetry of PD and the effective therapeutic window. Specifically, G8’s beta-band metric for the left STN was 4.25 mm. In PD, the neurodegenerative process often alters asymmetrically the dopaminergic innervation of the two striata; this leads to lateralized onset of motor symptoms with persisting asymmetry as the disease progresses [49]. We determined that in this patient, the most-affected side was the left one, being controlled by the right hemisphere. Hence, despite the DBS lead misplacement on the left STN, the positive clinical result was most probably due to the precise stimulation of the right STN, which is consistent with the small beta-band metric on that side. What is more, G9 exhibited large metrics bilaterally. Despite the substantial improvement in UPDRS, this patient suffered from a partial amelioration of PD symptoms and subsequent rise of stimulation-induced side effects (see Section II-C). The clinical picture and the large beta-band metrics are consistent with a narrow therapeutic window in which the side effects do not allow for a further increase of the stimulation current. Concerning the “poor” responders, P8 was reported to respond poorly in DBS as he developed dysarthrophonic speech and walking difficulty despite the addition of a second stimulation contact in a follow-up study (see Section II-C). Yet, his beta-band markers for the left (right) STN were -2.25 (0.75) mm, a metric that would be expected to found in “good” responders. The dysarthrophonic speech and the walking difficulty of the patient could possibly be explained by the spread of the stimulus to other, unrelated to movement, adjacent structures (i.e., cerebello-rubro-thalamic fibers); this might have put a constraint on the length of the therapeutic window as the stimulation current (and hence the brain tissue volume that this covers) could not increase to a therapeutic level.

In addition, there seems to be no clear connection between downward displacement of the stimulation lead and the poor DBS response as any downward displacement would result to a smaller, not larger, metric. Consider, for example, point_B in Fig. 1 and a stimulation lead downward displaced by X mm, $0 < X \leq 1.5$ [9]. The new distance_B = $d_2 - (d_1 + X) < d_2 - d_1$. In other words, if the lead displacement was the reason for the “poor” response, one would expect to find *smaller metrics* in poor response and, therefore, the difference in metrics between “poor” and “good” responders would not be significant.

Not only the presence of the beta peak but also the span of the beta oscillations, as estimated by our proposed marker, could potentially be used to decide upon the stimulation area. The maximum beta peak was found close to the stimulation contact depth, in most “good” responders. Multiple prominent beta-band peaks were also present in patients with two stimulation contacts. These results are supportive of testing our method with the next generation of deep brain stimulators that will no longer be a single stripe of four contacts but, instead,

will comprise of a 3-D array of contacts [50] that will adapt based on neurofeedback [51] after assessing the effect of their own stimulation in the surrounding tissue [52]. Localization of the most prominent beta peaks inside the STN could guide the *selective* stimulation of the areas that would be closest to the prominent beta peaks. However, since the pool of patients is small in this study, we need to extend it before we reach to general conclusions.

V. CONCLUSION

Our proposed method provides evidence that the optimal long-term motor-related DBS clinical results and the minimization of the side effects can be informed by the beta-band peaks acquired intraoperatively. When the stimulation was applied in close proximity to the spatial extent of the most prominent beta-oscillatory region, believed to overlap with the motor territories of the STN, PD patients responded well on DBS, for at least two years after surgery. This biophysical signature of long-term improvement after STN-DBS could prove useful in guiding clinical decisions on the best electrode trajectory intraoperatively and the best stimulation contact(s) during and after surgery.

REFERENCES

- [1] A. Benabid, P. Pollak, C. Gross, D. Hoffmann, A. Benazzouz, D. Gao *et al.*, “Acute and long-term effects of subthalamic nucleus stimulation in Parkinson’s disease,” *Stereotactic Funct. Neurosurg.*, vol. 62, pp. 76–84, 1994.
- [2] C. Hammond, R. Ammari, B. Bioulac, and L. Garcia, “Latest view on the mechanism of action of deep brain stimulation,” *Movement Disorders*, vol. 23, pp. 2111–2121, 2008.
- [3] P. Limousin, P. Krack, P. Pollak, A. Benazzouz, C. Ardouin, D. Hoffmann *et al.*, “Electrical stimulation of the subthalamic nucleus in advanced Parkinson’s disease,” *New Engl. J. Med.*, vol. 339, pp. 1105–1111, 1998.
- [4] E. Moro, M. Scerrati, L. Romito, R. Roselli, P. Tonali, and A. Albanese, “Chronic subthalamic nucleus stimulation reduces medication requirements in Parkinson’s disease,” *Neurology*, vol. 53, pp. 85–85, 1999.
- [5] P. Krack, V. Fraix, A. Mendes, A. L. Benabid, and P. Pollak, “Postoperative management of subthalamic nucleus stimulation for Parkinson’s disease,” *Movement Disorders*, vol. 17, pp. S188–S197, 2002.
- [6] J. Volkmann, J. Herzog, F. Kopper, and G. Deuschl, “Introduction to the programming of deep brain stimulators,” *Movement Disorders*, vol. 17, pp. S181–S187, 2002.
- [7] R. E. Gross, P. Krack, M. C. Rodriguez-Oroz, A. R. Rezai, and A. L. Benabid, “Electrophysiological mapping for the implantation of deep brain stimulators for Parkinson’s disease and tremor,” *Movement Disorders*, vol. 21, pp. S259–S283, 2006.
- [8] W. Hutchison, R. Allan, H. Opitz, R. Levy, J. Dostrovsky, A. Lang *et al.*, “Neurophysiological identification of the subthalamic nucleus in surgery for Parkinson’s disease,” *Ann. Neurol.*, vol. 44, pp. 622–628, 1998.
- [9] D. E. Sakas, A. T. Kouyialis, E. J. Boviatisis, I. G. Panourias, P. Stathis, and G. Tagaris, “Technical aspects and considerations of deep brain stimulation surgery for movement disorders,” *Acta Neurochirurgica Suppl.*, vol. 97, pp. 163–170, 2007.
- [10] Deep-Brain Stimulation for Parkinson’s Disease Study Group, “Deep-brain stimulation of the subthalamic nucleus or the pars interna of the globus pallidus in Parkinson’s disease,” *New Engl. J. Med.*, vol. 345, pp. 956–963, 2001.
- [11] A. Castrioto, J. Volkmann, P. Krack, M. AM Lozano, and E. Hallett, “Post-operative management of deep brain stimulation in Parkinson’s disease,” in *Handbook of Clinical Neurology, Brain Stimulation*, A. M. Lozano and M. Hallett Eds. Oxford, U.K.: Elsevier, 2013, pp. 129–146.
- [12] A. Moran, I. Bar-Gad, H. Bergman, and Z. Israel, “Real-time refinement of subthalamic nucleus targeting using Bayesian decision-making on the root mean square measure,” *Movement Disorders*, vol. 21, pp. 1425–1431, 2006.

- [13] P. Novak, S. Daniluk, S. A. Elias, and J. M. Nazzaro, "Detection of the subthalamic nucleus in microelectrographic recordings in Parkinson disease using the high-frequency (>500 Hz) neuronal background: Technical note," *J. Neurosurg.*, vol. 106, pp. 175–179, 2007.
- [14] A. Zaidel, A. Spivak, L. Shpigelman, H. Bergman, and Z. Israel, "Delimiting subterritories of the human subthalamic nucleus by means of microelectrode recordings and a hidden Markov model," *Movement Disorders*, vol. 24, pp. 1785–1793, 2009.
- [15] K. P. Michmizos, D. Sakas, and K. S. Nikita, "Toward relating the subthalamic nucleus spiking activity to the local field potentials acquired intranuclearly," *Meas. Sci. Technol.*, vol. 22, p. 114021, 2011.
- [16] K. P. Michmizos and K. S. Nikita, "Local field potential driven Izhikevich model predicts a subthalamic nucleus neuron activity," in *Proc. Annu. Int. Conf. Eng. Med. Biol. Soc.*, 2011, pp. 5900–5903.
- [17] K. P. Michmizos, K. S. Nikita, G. L. Tagaris, and D. E. Sakas, "Towards input output non-linear modeling of the subthalamic nucleus using intranuclear recordings," in *Proc. 4th Int. IEEE/EMBS Conf. Neural Eng.*, 2009, pp. 601–604.
- [18] K. P. Michmizos, D. Sakas, and K. S. Nikita, "Prediction of the timing and the rhythm of the Parkinsonian subthalamic nucleus neural spikes using the local field potentials," *IEEE Trans. Inf. Technol. Biomed.*, vol. 16, no. 2, pp. 190–197, Mar. 2012.
- [19] K. P. Michmizos and K. S. Nikita, "Addition of deep brain stimulation signal to a local field potential driven Izhikevich model masks the pathological firing pattern of an STN neuron," in *Proc. Annu. Int. Conf. IEEE Eng. Med. Biol. Soc.*, 2011, pp. 7290–7293.
- [20] C. C. Chen, A. Pogosyan, L. U. Zrinzo, S. Tisch, P. Limousin, K. Ashkan, et al., "Intra-operative recordings of local field potentials can help localize the subthalamic nucleus in Parkinson's disease surgery," *Exp. Neurol.*, vol. 198, pp. 214–221, 2006.
- [21] T. Trottenberg, N. Fogelson, A. A. Kühn, A. Kivi, A. Kupsch, G.-H. Schneider, et al., "Subthalamic gamma activity in patients with Parkinson's disease," *Exp. Neurol.*, vol. 200, pp. 56–65, 2006.
- [22] P. Brown, A. Oliviero, P. Mazzone, A. Insola, P. Tonali, and V. Di Lazzaro, "Dopamine dependency of oscillations between subthalamic nucleus and pallidum in Parkinson's disease," *J. Neurosci.*, vol. 21, pp. 1033–1038, 2001.
- [23] A. Moran, H. Bergman, Z. Israel, and I. Bar-Gad, "Subthalamic nucleus functional organization revealed by Parkinsonian neuronal oscillations and synchrony," *Brain*, vol. 131, pp. 3395–3409, 2008.
- [24] M. Cassidy, P. Mazzone, A. Oliviero, A. Insola, P. Tonali, V. Di Lazzaro, et al., "Movement-related changes in synchronization in the human basal ganglia," *Brain*, vol. 125, pp. 1235–1246, 2002.
- [25] A. A. Kühn, D. Williams, A. Kupsch, P. Limousin, M. Hariz, G. H. Schneider, et al., "Event-related beta desynchronization in human subthalamic nucleus correlates with motor performance," *Brain*, vol. 127, pp. 735–746, 2004.
- [26] G. Giannicola, S. Marceglia, L. Rossi, S. Mrakic-Sposta, P. Rampini, F. Tamma, et al., "The effects of levodopa and ongoing deep brain stimulation on subthalamic beta oscillations in Parkinson's disease," *Exp. Neurol.*, vol. 226, pp. 120–127, 2010.
- [27] B. Wingeier, T. Tcheng, M. M. Koop, B. C. Hill, G. Heit, and H. M. Bronte-Stewart, "Intra-operative STN DBS attenuates the prominent beta rhythm in the STN in Parkinson's disease," *Exp. Neurol.*, vol. 197, pp. 244–251, 2006.
- [28] P. A. Starr, "Placement of deep brain stimulators into the subthalamic nucleus or globus pallidus internus: Technical approach," *Stereotact. Funct. Neurosurg.*, vol. 79, pp. 118–145, 2003.
- [29] H. Cagnan, K. Dolan, X. He, M. F. Contarino, R. Schuurman, P. van den Munckhof, et al., "Automatic subthalamic nucleus detection from microelectrode recordings based on noise level and neuronal activity," *J. Neural Eng.*, vol. 8, p. 046006, 2011.
- [30] K. A. Nestor, J. D. Jones, C. R. Butson, T. Morishita, C. E. Jacobson IV, D. A. Peace, et al., "Coordinate-based lead location does not predict Parkinson's disease deep brain stimulation outcome," *PLoS One*, vol. 9, p. e93524, 2014.
- [31] G. L. Defer, H. Widner, R. M. Marié, P. Rémy, and M. Levivier, "Core assessment program for surgical interventional therapies in Parkinson's disease (CAPSIT-PD)," *Movement Disorders*, vol. 14, pp. 572–584, 1999.
- [32] P. A. Starr, C. W. Christine, P. V. Theodosopoulos, N. Lindsey, D. Byrd, A. Mosley, et al., "Implantation of deep brain stimulators into the subthalamic nucleus: Technical approach and magnetic resonance imaging-verified lead locations," *J. Neurosurg.*, vol. 97, pp. 370–387, Aug. 2002.
- [33] M. F. Contarino, M. Bot, J. D. Speelman, R. M. de Bie, M. A. Tijssen, D. Denys, et al., "Postoperative displacement of deep brain stimulation electrodes related to lead-anchoring technique," *Neurosurgery*, vol. 73, pp. 681–688, 2013.
- [34] J. Volkmann, E. Moro, and R. Pahwa, "Basic algorithms for the programming of deep brain stimulation in Parkinson's disease," *Movement Disorders*, vol. 21, pp. S284–S289, 2006.
- [35] P. D. Welch, "The use of fast Fourier transform for the estimation of power spectra: A method based on time averaging over short, modified periodograms," *IEEE Trans. Audio Electroacoust.*, vol. AU-15, no. 2, pp. 70–73, Jun. 1967.
- [36] K. P. Michmizos, D. Sakas, and K. S. Nikita, "Parameter identification for a local field potential driven model of the Parkinsonian subthalamic nucleus spike activity," *Neural Netw.*, vol. 36, pp. 146–156, 2012.
- [37] D. J. Sheskin, *Handbook of Parametric and Nonparametric Statistical Procedures*. Boca Raton, FL, USA: CRC Press, 2003.
- [38] G. Kleiner-Fisman, J. Herzog, D. N. Fisman, F. Tamma, K. E. Lyons, R. Pahwa, et al., "Subthalamic nucleus deep brain stimulation: Summary and meta-analysis of outcomes," *Movement Disorders*, vol. 21, pp. S290–S304, 2006.
- [39] M. Rodriguez-Oroz, J. Obeso, A. Lang, J.-L. Houeto, P. Pollak, S. Rehncrona, et al., "Bilateral deep brain stimulation in Parkinson's disease: A multicentre study with 4 years follow-up," *Brain*, vol. 128, pp. 2240–2249, 2005.
- [40] C. G. Goetz, B. C. Tilley, S. R. Shaftman, G. T. Stebbins, S. Fahn, P. Martinez-Martin, et al., "Movement disorder society-sponsored revision of the unified Parkinson's disease rating scale (MDS-UPDRS): Scale presentation and clinimetric testing results," *Movement Disorders*, vol. 23, pp. 2129–2170, 2008.
- [41] A. Antonini, G. Marotta, R. Benti, A. Landi, R. De Notaris, C. Mariani, et al., "Brain flow changes before and after deep brain stimulation of the subthalamic nucleus in Parkinson's disease," *Neurol. Sci.*, vol. 24, pp. 151–152, Oct. 2003.
- [42] J. Herzog, U. Fietzek, W. Hamel, A. Morsnowski, F. Steigerwald, B. Schrader, et al., "Most effective stimulation site in subthalamic deep brain stimulation for Parkinson's disease," *Movement Disorders*, vol. 19, pp. 1050–1054, 2004.
- [43] C. Bedard, H. Kröger, and A. Destexhe, "Model of low-pass filtering of local field potentials in brain tissue," *Phys. Rev. E*, vol. 73, p. 051911, 2006.
- [44] A. Zaidel, A. Spivak, B. Grieb, H. Bergman, and Z. Israel, "Subthalamic span of β oscillations predicts deep brain stimulation efficacy for patients with Parkinson's disease," *Brain*, vol. 133, pp. 2007–2021, 2010, Paper awq144.
- [45] F. Amtege, K. Henschel, B. Schelter, J. Vesper, J. Timmer, C. H. Lücking, et al., "High functional connectivity of tremor related subthalamic neurons in Parkinson's disease," *Clin. Neurophysiol.*, vol. 120, pp. 1755–1761, 2009.
- [46] A. Eusebio and P. Brown, "Synchronisation in the beta frequency-band—The bad boy of Parkinsonism or an innocent bystander?" *Exp. Neurol.*, vol. 217, pp. 1–3, 2009.
- [47] A. A. Kühn, A. Tsui, T. Aziz, N. Ray, C. Brücke, A. Kupsch, et al., "Pathological synchronisation in the subthalamic nucleus of patients with Parkinson's disease relates to both bradykinesia and rigidity," *Exp. Neurol.*, vol. 215, pp. 380–387, 2009.
- [48] J. B. Toledo, J. López-Azcárate, D. Garcia-Garcia, J. Guridi, M. Valencia, J. Artieda, et al., "High beta activity in the subthalamic nucleus and freezing of gait in Parkinson's disease," *Neurobiol. Dis.*, vol. 64, pp. 60–65, 2014.
- [49] K. Marek, J. Seibyl, S. Zoghbi, Y. Zea-Ponce, R. Baldwin, B. Fussell, et al., "[sup 123 I] beta-CIT/SPECT imaging demonstrates bilateral loss of dopamine transporters in hemi-Parkinson's disease," *Neurology*, vol. 46, pp. 231–237, 1996.
- [50] P. S. Motta and J. W. Judy, "Multielectrode microprobes for deep-brain stimulation fabricated with a customizable 3-D electroplating process," *IEEE Trans. Biomed. Eng.*, vol. 52, no. 5, pp. 923–933, May 2005.
- [51] F. D. Broccard, T. Mullen, Y. M. Chi, D. Peterson, J. R. Iversen, M. Arnold, et al., "Closed-loop brain-machine-body interfaces for noninvasive rehabilitation of movement disorders," *Ann. Biomed. Eng.*, vol. 42, pp. 1573–1593, 2014.
- [52] C. Schmidt and U. van Rienen, "Modeling the field distribution in deep brain stimulation: The influence of anisotropy of brain tissue," *IEEE Trans. Biomed. Eng.*, vol. 59, no. 6, pp. 1583–1592, Jun. 2012.

Authors' photographs and biographies not available at the time of publication.